

RESEARCH ARTICLE

The role of observed cloud-radiative anomalies for the dynamics of the North Atlantic Oscillation on synoptic time-scales

Georgios Papavasileiou¹  | Aiko Voigt^{1,2}  | Peter Knippertz¹ 

¹Institute of Meteorology and Climate Research, Karlsruhe Institute of Technology (KIT), Karlsruhe, Germany

²Lamont-Doherty Earth Observatory, Columbia University, New York, USA

Correspondence

G. Papavasileiou, Department of Troposphere Research, Institute of Meteorology and Climate Research, Karlsruhe Institute of Technology, 76131 Karlsruhe, Germany
Email: georgios.papavasileiou@kit.edu

Funding information

German Ministry of Education and Research (BMBF) and Research for Sustainable Development (FONA), Grant/Award Number: 01LK1509A; Transregional Collaborative Research Centre SFB/TRR 165 “Waves to Weather” of the German Research Foundation (DFG)

[Correction added on 8 April 2020, after first online publication. Additional funding information has been included in this version of the article.]

Abstract

Clouds shape weather and climate by regulating the latent and radiative heating in the atmosphere. Recent work has demonstrated the importance of cloud-radiative effects (CRE) for the mean circulation of the extratropical atmosphere and its response to global warming. In contrast, little research has been done regarding the impact of CRE on internal variability. Here, we study how clouds and the North Atlantic Oscillation (NAO) couple on synoptic time-scales during Northern Hemisphere winter via CRE within the atmosphere (ACRE). A regression analysis based on 5-day mean data from CloudSat/CALIPSO, CERES and GERB satellite observations and ERA-Interim short-term forecast data reveals a robust dipole of high-level and low-level cloud-incidence anomalies during a positive NAO, with increased high-level cloud incidence along the storm track (near 45°N) and the subpolar Atlantic, and decreased high-level cloud incidence poleward and equatorward of this track. Opposite changes occur for low-level cloud incidence. The cloud anomalies lead to an anomalous column-mean heating from ACRE over the region of the Iceland low, and to a cooling over the region of the Azores high. To quantify the impact of the ACRE anomalies on the NAO, and to thereby test the hypothesis of a cloud-radiative feedback on the NAO persistence, we apply the surface pressure tendency equation for ERA-Interim short-term forecast data. The NAO-generated ACRE anomalies amplify the NAO-related surface pressure anomalies over the Azores high but have no area-averaged impact on the Iceland low. In contrast, diabatic processes as a whole, including latent heating and clear-sky radiation, strongly amplify the NAO-related surface pressure anomalies over both the Azores high and the Iceland low, and their impact is much more spatially coherent. This suggests that, while atmospheric cloud-radiative effects lead to an increase in NAO persistence on synoptic time-scales, their impact is relatively minor and much smaller than other diabatic processes.

KEYWORDS

atmospheric cloud-radiative effects (ACRE), cloud-circulation coupling, diabatic processes, latent heating, North Atlantic Oscillation (NAO)

This is an open access article under the terms of the Creative Commons Attribution License, which permits use, distribution and reproduction in any medium, provided the original work is properly cited.

© 2020 The Authors. *Quarterly Journal of the Royal Meteorological Society* published by John Wiley & Sons Ltd on behalf of the Royal Meteorological Society.

1 | INTRODUCTION

The weather and climate of the North Atlantic region and the neighbouring North American and European continental areas exhibit considerable variability on a wide range of spatiotemporal scales. A large part of this variability is explained by the North Atlantic Oscillation (NAO; Hurrell, 1995; Visbeck *et al.*, 2001; Hurrell *et al.*, 2003), which is a surface pressure seesaw with centres of action near Iceland and around the Azores. The NAO is the dominant mode of atmospheric variability over the North Atlantic and the surrounding continental areas of North America and Europe during winter (Wanner *et al.*, 2001; Visbeck *et al.*, 2001; Hurrell and Deser, 2010). It modulates the latitudinal position of the eddy-driven jet and the storm track (Woollings *et al.*, 2010), and extreme and persistent NAO states are associated with high-impact weather events (Scaife *et al.*, 2008). The observational work of Li *et al.* (2014a) hypothesised that cloud-radiative effects (CRE) might represent an important and so far overlooked factor for the NAO and its variability. Here, we investigate this hypothesis in more detail by combining a suite of satellite observations, reanalysis data, and a dynamical analysis based on the surface pressure tendency equation.

On synoptic time-scales the NAO arises as an internal mode of the tropospheric circulation from eddy-mean flow interactions (Hurrell *et al.*, 2003; Thompson *et al.*, 2003; Barnes and Hartmann, 2010). External forcings such as the stratosphere (Baldwin and Dunkerton, 1999; Ambaum and Hoskins, 2002; Kidston *et al.*, 2015), the ocean (Visbeck, 2002) and sea-ice (Krahmann and Visbeck, 2003; Semenov and Latif, 2015) can also play a role. The persistence of the NAO, or more generally the annular modes and the extratropical jet streams, was examined from the perspective of the adiabatic circulation and dynamical feedbacks involving eddies (Lorenz and Hartmann, 2001; 2003; Barnes and Hartmann, 2010). Diabatic processes, such as latent heating, can modify the NAO persistence (Greatbatch and Jung, 2007; Xia and Chang, 2014; Woollings *et al.*, 2016).

There is reason to believe that, besides latent heating, radiative heating from clouds can affect the NAO persistence. This idea is motivated by observational and modelling studies that highlighted the close coupling between CRE and the extratropical circulation across a range of time-scales. This includes observational studies that have shown the impact of the extratropical circulation, i.e. the position of the extratropical jet, static stability and large-scale vertical motion, on the patterns of cloud and CRE based on internal circulation variability on time-scales of days to weeks (Grise *et al.*, 2013; Grise and Polvani, 2014; Li *et al.*, 2014b; Grise and Medeiros, 2016; Tselioudis *et al.*, 2016; Zelinka *et al.*, 2018). The

modelling work of Li *et al.* (2015) and Watt-Meyer and Frierson (2017) showed how CRE within the atmosphere (ACRE) modulate the mean position of the extratropical jet in the present-day climate. Other modelling work highlighted the importance of both atmospheric and surface CRE for the extratropical circulation response in model simulations of global warming (Voigt and Shaw, 2015; 2016; Ceppi and Hartmann, 2016; Albern *et al.*, 2019; Li *et al.*, 2019; Voigt *et al.*, 2019). As a whole, these studies illustrate the need for understanding and constraining the radiative impact of clouds on the circulation (Bony *et al.*, 2015). This need is exacerbated by the difficulties of current global climate models to adequately represent clouds and their radiative effects.

While the importance of CRE for the present-day mean circulation of the extratropics and its long-term climate change response is well established, at least from a modelling perspective, little research has been done regarding a possible impact of CRE on the extratropical circulation on synoptic time-scales. Schäfer and Voigt (2018) proposed that CRE weaken idealised extratropical cyclones, which would seem to suggest a possible impact on storm tracks, the jet stream, and hence the NAO. Grise *et al.* (2019) found that CRE lead to a small but statistically significant weakening of extratropical storm tracks and cyclones. Li *et al.* (2014a) investigated the relation between clouds and the Arctic Oscillation (to which they refer as the Northern Annular Mode/North Atlantic Oscillation; NAM/NAO) on monthly time-scales using satellite observations and reanalysis data. They found that the NAM/NAO is associated with robust changes in high-level clouds and top-of-atmosphere CRE, which in the zonal mean works against the temperature anomalies accompanying the NAM/NAO. Li *et al.* (2014a) interpreted this as a negative cloud-radiative feedback that shortens the NAM/NAO time-scale. Over the North Atlantic region, however, evidence for a negative cloud-radiative feedback only emerged in the lower midlatitude region near the Azores. This, and the fact that the North Atlantic storm track and jet stream are tilted meridionally, suggests that a regional latitude-longitude perspective is warranted.

In this study, we build upon the work of Li *et al.* (2014a). We clarify the role of CRE within the atmosphere (ACRE) for the NAO variability on synoptic time-scales. We use 5-day means, in contrast to the monthly means considered by Li *et al.* (2014a). This allows us to compare more directly the cloud impact with the impact of synoptic eddies, and the larger sample size helps us identify statistically significant signals (Li and Thompson, 2016). We base our analysis on essentially the same observational and reanalysis data as in Li *et al.* (2014a), but make use of the NAO instead of the AO index, so as to focus on circulation variability in the North Atlantic region.

Also, because radiative processes associated with changes in surface air temperatures are not expected to impact sea surface temperatures over the synoptic time-scales that we consider here, we focus on ACRE instead of top-of-atmosphere CRE. We consider the winter months of December–January–February, whereas Li *et al.* (2014a) analysed the extended winter from October to March.

In Section 2 we detail the observational and reanalysis datasets that we use to identify the impact of the NAO on clouds and CRE. In Section 3 we present results from the analysis of the observational datasets. In Section 4 we repeat this analysis using reanalysis datasets, and further quantify the impact of CRE on NAO variability using the surface pressure tendency equation. This analysis also allows us to compare the impact of CRE to the impact of the dynamics and diabatic processes as a whole. In Section 5 we compare our results with Li *et al.* (2014a). The paper finishes with conclusions in Section 6.

2 | SATELLITE OBSERVATIONS, NAO INDEX AND REANALYSIS DATA

2.1 | CloudSat/CALIPSO cloud incidence

We use cloud observations for years 2006 to 2011 from the 2B-GEOPROF-LIDAR product (version P2R04; Mace *et al.*, 2009), which combines CloudSat Cloud Profiling Radar (CPR) and Cloud-Aerosol Lidar and Infrared Pathfinder Satellite Observation (CALIPSO) lidar retrievals. CloudSat's CPR is a non-scanning nadir-pointing space-borne radar operating at 94 GHz frequency and provides reflectivity profiles within 82° N/S with along- and cross-track horizontal resolutions of about 1.7 and 1.4 km respectively and a vertical resolution of 240 m (Tanelli *et al.*, 2008; Verlinden *et al.*, 2011).

We analyse cloud incidence. Cloud incidence is the likelihood that within a given atmospheric volume the satellite senses a cloud. We calculate cloud incidence following Verlinden *et al.* (2011) and Li *et al.* (2014a). Due to the spatiotemporal limitations of CloudSat/CALIPSO on daily time-scales (Mace *et al.*, 2009; Li *et al.*, 2014a), we bin the vertical profiles into a 2.5° (longitude) x 2.5° (latitude) x 240 m (vertical) grid, and average the binned data over time periods of 5 days.

2.2 | CloudSat/CALIPSO cloud-radiative effects

We use the CloudSat/CALIPSO 2B-FLXHR-LIDAR product over the time period 2006–2011 (version P2R04; L'Ecuyer *et al.*, 2008; Henderson *et al.*, 2013). The

2B-FLXHR-LIDAR product is based on radiative transfer calculations that make use of the CloudSat/CALIPSO cloud retrievals and allows for a detailed look at the vertical structure of atmospheric cloud-radiative effects (ACRE). ACRE at a given atmospheric pressure level are defined as the all-sky minus the clear-sky radiative heating rates (in units of K·day⁻¹). We compute the all-sky and clear-sky radiative heating rates from the long-wave and short-wave radiative fluxes (in units of W·m⁻²) at every 240 m height level provided by 2B-FLXHR-LIDAR.

ACRE measures the impact of cloud-radiative heating/cooling on atmospheric temperatures and is calculated as (Haynes *et al.*, 2013)

$$\left. \frac{dT}{dt} \right|_{\text{CRE}} = \left. \frac{dT}{dt} \right|_{\text{all-sky}} - \left. \frac{dT}{dt} \right|_{\text{clear-sky}}, \quad (1)$$

where the all-sky and clear-sky heating rates are calculated as

$$\left. \frac{dT}{dt} \right|_{\text{all-sky/clear-sky}} = -\frac{1}{\rho c_p} \frac{dF_{\text{all-sky/clear-sky}}}{dz}. \quad (2)$$

T is the air temperature and ρ is the air density from the ECMWF-AUX product (CIRA, 2007), c_p is the specific heat of dry air at constant pressure, z is altitude, and t is time. ACRE is binned in the same way as cloud incidence and averaged over time periods of 5 days. Vertically integrated ACRE is calculated from the difference of top-of-atmosphere (TOA) and bottom-of-atmosphere (BOA) fluxes provided by the 2B-FLXHR-LIDAR product and is expressed in units of W·m⁻².

2.3 | CERES and GERB/SEVIRI cloud-radiative effects

To test the robustness of the CloudSat/CALIPSO results we also analyse CERES (Clouds and Earth's Radiant Energy System) and GERB/SEVIRI (Geostationary Earth Radiation Budget/Spinning Enhanced Visible and InfraRed Imager) observations of TOA and BOA cloud-radiative effects.

We use CERES-SYN1deg edition 4A (Rutan *et al.*, 2015) for daily-mean CRE at the TOA and BOA. Apart from CERES observations, CERES-SYN1deg makes use of cloud observations from MODIS and geostationary satellites, and CRE at the BOA are derived from radiative transfer calculations. Again, we calculate the vertically integrated ACRE from the CRE difference at the TOA and BOA. We use CERES-SYN1deg for the same 2006 to 2011 period for which CloudSat/CALIPSO is available, as well as for a longer period from years 2000 to 2017.

We further use monthly mean fields from CERES-EBAF (Energy Balanced and Filled) edition 4.0

(Loeb *et al.*, 2018) for years 2002 to 2017 and from GERB/SEVIRI (Harries *et al.*, 2005) for years 2006–2011. For CERES-EBAF we analyse long-wave and short-wave CRE at the TOA and BOA, from which we derive vertically integrated ACRE. For GERB/SEVIRI, we use TOA and BOA all-sky and clear-sky long-wave radiative fluxes. TOA fluxes are available at 0.1° spatial resolution, while BOA fluxes are available at 0.05° . We remap the fluxes onto a common 0.1° grid and derive TOA and BOA long-wave CRE as well as vertically integrated long-wave ACRE.

2.4 | North Atlantic Oscillation index

We use daily values of the NAO index provided by the National Oceanic and Atmospheric Administration Climate Prediction Centre (NOAA-CPC). The index is based on the anomalous geopotential height at 500 hPa. Normalised daily values are available from year 1950 onwards and can be downloaded from <ftp://ftp.cpc.ncep.noaa.gov/cwlinks/> (accessed 24 February 2020). For the regression analyses presented below, the NAO is standardised to a standard deviation of 1.

2.5 | ERA-Interim

We use short-term forecasts from the ERA-Interim reanalysis dataset in full spatial resolution T255 (0.75° grid spacing). ERA-Interim was generated by the European Centre for Medium-Range Weather Forecasts (ECMWF) covering the time period from 1979 to 2019 (Dee *et al.*, 2011). We use short-term forecasts because some of the input data for our analysis of the surface pressure tendency equation in Section 4, e.g., the radiative heating rates, are only available in the forecast. The 4D-variational data assimilation scheme of ERA-Interim makes use of a time window of 12 hr. This means that the short-term forecasts are strongly tied to the analysis and hence observations, implying that there is substantial knowledge of the synoptic-scale features. Given that the diabatic processes are not directly observed, we have no alternative to using model-generated fields (also Maranan *et al.*, 2019).

We study two periods, 2006–2011 and 1979–2017. Our use of ERA-Interim serves two purposes. First, it supplements the satellite observations by means of cloud fraction and ACRE derived from accumulated TOA and BOA radiative fluxes in all-sky and clear-sky conditions in the 6- and 12-hr forecasts initialised from the analyses at 0000 and 1200 UTC. Six-hourly means of radiative fluxes are derived from the accumulated fluxes by (a) dividing the 6-hr accumulated flux by the time period of 6 hr, and (b) by differencing the 12- and 6-hr accumulated fluxes and

then also dividing by 6 hr. Given the different treatment of clouds in models and satellite data, we do not aim to validate ERA-Interim, but rather look for broad consistency between the complementary sources of information. We remind the reader that cloud cover from ERA-Interim and cloud incidence from CloudSat/CALIPSO should not be compared quantitatively because of different treatments of cloud overlap. Second, we use ERA-Interim for the surface pressure tendency analysis. Six-hourly snapshot values of wind, temperature, geopotential height, humidity and surface pressure are taken from the 6- and 12-hr forecasts initialised from the analyses at 0000 and 1200 UTC. For evaporation, precipitation and the temperature tendencies from ACRE, clear-sky radiative heating, and the sum of all diabatic processes, we use accumulated fields from the 6- and 12-hr forecasts and convert these to 6-hourly means in the same manner as described above for radiative fluxes.

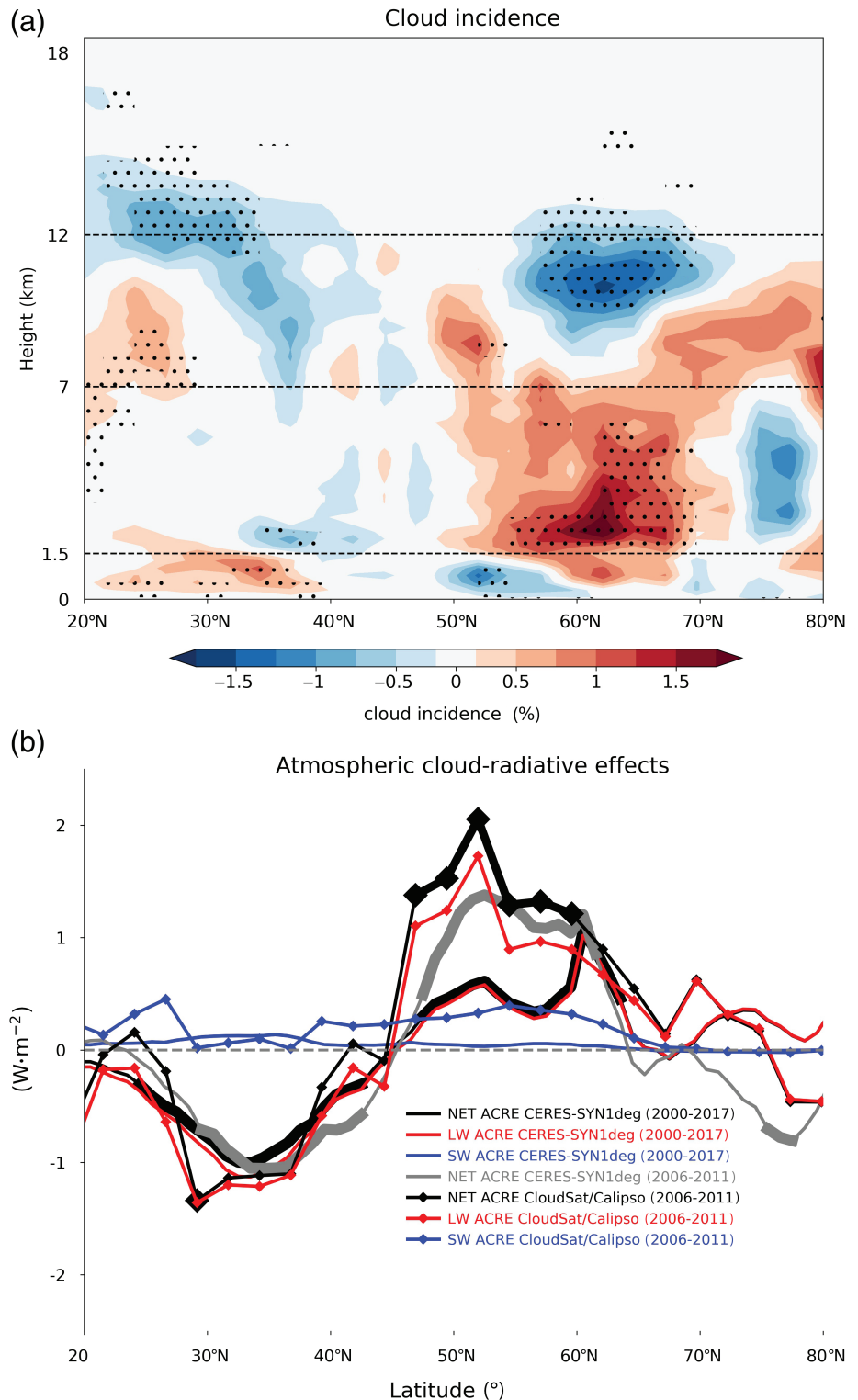
3 | NAO IMPACT ON CLOUDS AND ACRE IN SATELLITE OBSERVATIONS

In this section we study the NAO impact on clouds and ACRE in satellite observations by means of linear regressions of 5-day means (for CloudSat/CALIPSO and CERES-SYN1deg) or monthly means (for CERES-EBAF and GERB/SEVIRI). We start with an analysis of the zonal mean and then proceed with a latitude–longitude view over the North Atlantic region. We further analyse vertical profiles over the two domains around the Iceland low and Azores high, which are the centres of action of the NAO sea-level pressure seesaw.

3.1 | Zonal-mean perspective

Motivated by the zonal-mean analysis of Li *et al.* (2014a), we start with studying the NAO impact on zonal-mean cloud incidence and ACRE in the Northern Hemisphere ($20\text{--}80^\circ\text{N}$) for 5-day means. Figure 1a shows regressions of zonal-mean cloud incidence from CloudSat/CALIPSO onto the NAO. During its positive phase, the higher midlatitudes ($55\text{--}70^\circ\text{N}$) experience a statistically significant decrease in high-level cloud incidence around 10 km and an increase in mid-level cloud incidence around 5 km. Further equatorward, low-level cloud incidence is increased in the subtropics and lower midlatitudes ($20\text{--}40^\circ\text{N}$), and around 25°N cloud incidence is increased around 8 km and decreased around 12 km. These findings are very similar to those of Li and Thompson (2016), who calculated year-round regressions (their figure 2d).

FIGURE 1 NAO regression of DJF 5-day mean zonal-mean (a) cloud incidence from CloudSat/CALIPSO from 2006–2011 and (b) vertically integrated ACRE from CloudSat/CALIPSO during 2006–2011 (black with diamond marker) as well as from CERES-SYN1deg during 2006–2011 (grey) and 2000–2017 (black). The long-wave (LW) and short-wave (SW) components are also shown. Stippling in (a) and a thick line in (b) indicate statistical significance at the 5% level according to a two-sided Wald test



However, the NAO impact on zonal-mean cloud incidence is small and not statistically significant in most regions. This indicates that the zonal-mean perspective is of limited use to understand the NAO impact on the cloud pattern.

The NAO impact on zonal-mean vertically integrated ACRE from CloudSat/CALIPSO (2006–2011) and

CERES-SYN1deg (2006–2011 and 2000–2017) exhibits a much clearer and statistically significant meridional pattern (Figure 1b). During a positive phase of the NAO, ACRE decreases in the subtropics and lower midlatitudes (equatorward of 45°N), and increases in the higher midlatitudes between 50 and 65°N. The anomalies in ACRE are dominated by the long-wave component. The

heating dipole of subtropical and lower-midlatitude cooling and higher-midlatitude warming is robust in both CloudSat/CALIPSO and CERES-SYN1deg, which agree well for the time period between 2006 and 2011. Despite some decadal-scale variability in the magnitude of the NAO impact on higher midlatitude ACRE (compare the 2006–2011 and 2000–2017 periods in CERES-SYN1deg), the heating dipole is robust with respect to the observational time period and consistent with previous findings of Li *et al.* (2014a) (compare our Figure 1b with figure 2e of Li *et al.*, 2014a).

There is no clear relationship between the changes in zonal-mean cloud incidence, which are small and have a complex vertical structure, and the robust dipole in ACRE changes. In the following, we therefore change to a regional latitude–longitude perspective and investigate the NAO impact on clouds and ACRE specifically over the North Atlantic region.

3.2 | Latitude–longitude perspective over the North Atlantic region

The North Atlantic jet stream is tilted from southwest to northeast, different from the more zonally oriented jet streams in the North Pacific and the Southern Hemisphere. The tilt of the North Atlantic jet stream suggests that the NAO leads to zonally asymmetric cloud anomalies over the North Atlantic. This indicates that instead of a zonal mean, a latitude–longitude perspective is necessary.

The regression analysis reveals a rich pattern of the NAO impact on cloud incidence at different levels over the North Atlantic (Figure 2). At higher levels (7–12 km; Figure 2a), a positive phase of the NAO leads to increased cloud incidence along the storm track region (around 45°N; also Athanasiadis *et al.*, 2010) from eastern Canada/USA to Scandinavia and over the subpolar Atlantic. Decreased cloud incidence is evident in near-zonal bands from southwest of the Azores to the eastern Mediterranean and from the Labrador Sea to Iceland.

At mid-levels (1.5–7 km; Figure 2b), cloud incidence is increased poleward of the storm track over the eastern part of Greenland and over the subpolar North Atlantic. At the same time, the lower midlatitudes experience reduced mid-level cloud incidence during a positive NAO.

At lower levels (0–1.5 km; Figure 2c) the NAO impact on cloud incidence is opposite to that at high levels for many regions. Specifically, a positive NAO leads to increased low-level cloud incidence around the Azores and around the Labrador Sea, and decreased low-level cloud incidence in an area south of Iceland that extends from the Irminger Sea to Scandinavia.

The NAO impact on cloud incidence is in line with changes in large-scale static stability and vertical motion accompanying the NAO (Li *et al.*, 2014a; Grise and Medeiros, 2016; Li and Thompson, 2016). For example, the increase in high-level cloud incidence along the storm track region is consistent with large-scale ascent and the formation and eastward propagation of extratropical cyclones. The decrease in high-level and increase in low-level cloud incidence around the Azores is consistent with a strengthening of the high-pressure system and large-scale descent.

The NAO also impacts vertically integrated ACRE. For a positive NAO, changes in ACRE as derived from CloudSat/CALIPSO (Figure 2d) show a tilted meridional heating dipole along the southwest–northeast axis, with warming in a broad area around the British Isles and cooling in a broad area around the Azores. ACRE from CERES-SYN1deg shows a consistent impact of the NAO with higher statistical significance, thanks to the better spatio-temporal coverage of CERES-SYN1deg (Figure 2e for years 2006–2011; Figure 2f for years 2000–2017). The ACRE changes are characterised by a quadrupole that consists of heating east off the coast of Nova Scotia as well as over the eastern North Atlantic, the British Isles and Scandinavia, and cooling over the Azores and the Mediterranean as well as the Labrador Sea.

The quadrupole of the ACRE anomalies is consistent with the NAO impact on high- and low-level cloud incidence (Oreopoulos *et al.*, 2017). In many areas anomalous heating is associated with an increase in high-level cloud incidence and a decrease in low-level cloud incidence. Likewise, anomalous cooling is associated with a decrease in high-level cloud incidence and an increase in low-level cloud incidence.

3.3 | Vertical structure over Iceland and the Azores

We now analyse the vertical structure of cloud incidence and ACRE from CloudSat/CALIPSO over the two centres of actions of the NAO sea-level pressure seesaw, namely Iceland and the Azores. The Iceland and Azores domains are shown in Supporting Figure S1 and are selected based on NAO regressions of 5-day mean surface pressure from ERA-Interim. The Iceland domain contains areas with a surface pressure anomaly of at least -9.3 hPa. Because the absolute magnitude of the regression over Iceland is 1.9 times larger than over the Azores, a lower threshold of surface pressure anomalies of 4.9 hPa is chosen for the Azores domain. Moreover, to avoid spurious effects due to orography, land areas in the Iceland domain are neglected.

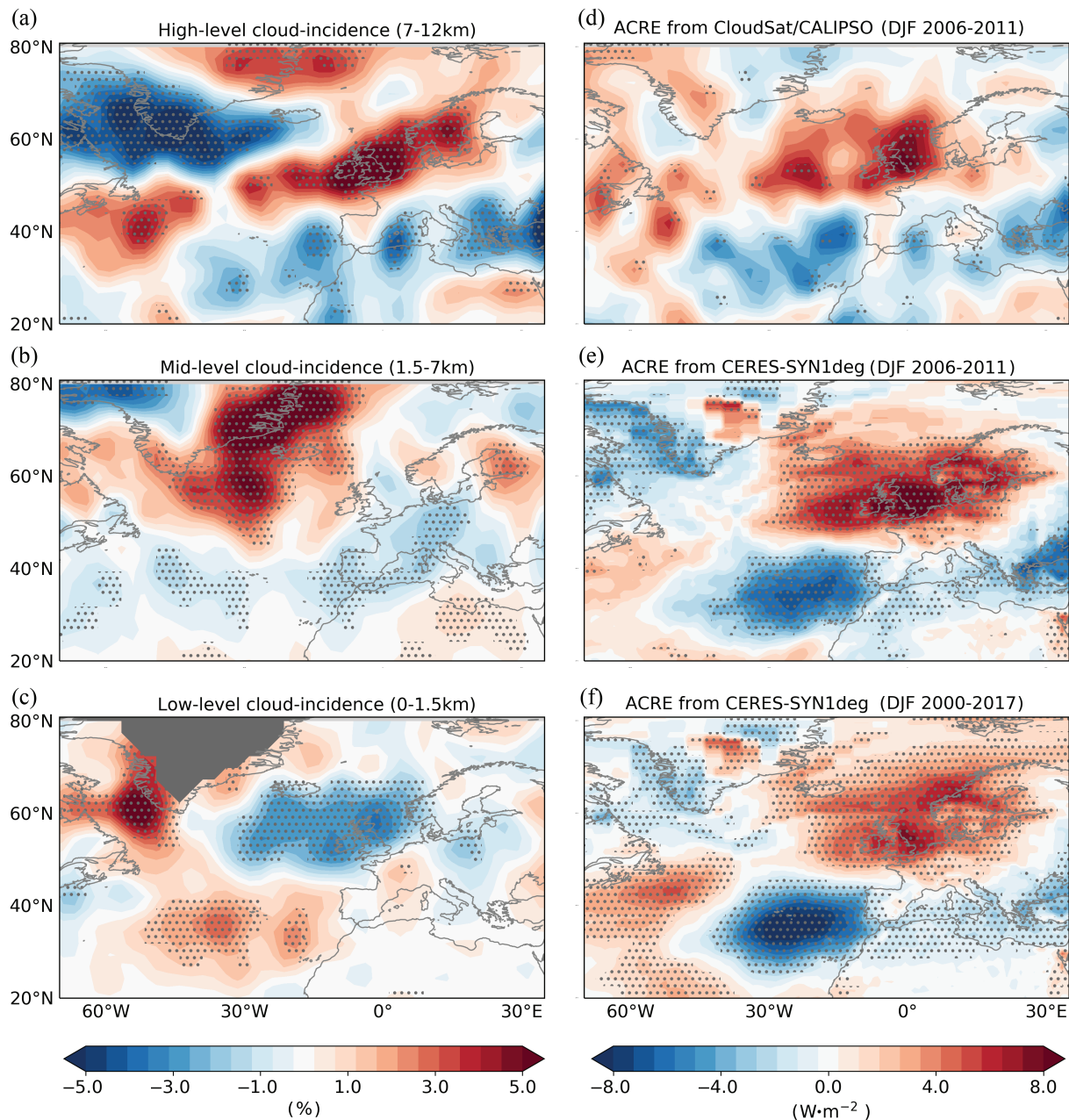


FIGURE 2 (a–c) NAO regression of DJF 5-day mean cloud incidence from CloudSat/CALIPSO from 2006–2011 for (a) high-, (b) mid- and (c) low-level clouds over the North Atlantic region. (d–f) NAO regressions of DJF 5-day mean vertically integrated ACRE for (d) CloudSat/CALIPSO during 2006–2011, and for CERES-SYN1deg during (e) 2006–2011 and (f) 2000–2017. Stippling indicates statistical significance at the 5% level according to a two-sided Wald test. For low-level clouds, Greenland is masked out. The CloudSat/CALIPSO data are smoothed using the 9-point smoothing function from the Climate Data Operator

3.3.1 | Iceland

Figure 3a,b show cloud incidence and ACRE averaged over the Iceland domain. The climatological cloud incidence exhibits two maxima; an upper-level maximum at 7 km and a low-level maximum at 1.5 km (Figure 3a, black). This leads to climatological cooling from ACRE around the high-level and low-level cloud tops, and heating at the bottom of low-level clouds (Figure 3b, black).

The impact of the NAO is on the order of 20% of the climatological value for cloud incidence (Figure 3a, blue), and up to 80% for ACRE (Figure 3b, red). During a positive phase of the NAO, high-level cloud incidence is decreased, and mid-level cloud incidence is increased. There is also an indication of decreased low-level cloud incidence. These changes indicate a downward shift of the climatological upper-level maximum in cloud incidence, probably a consequence of a lowered tropopause,

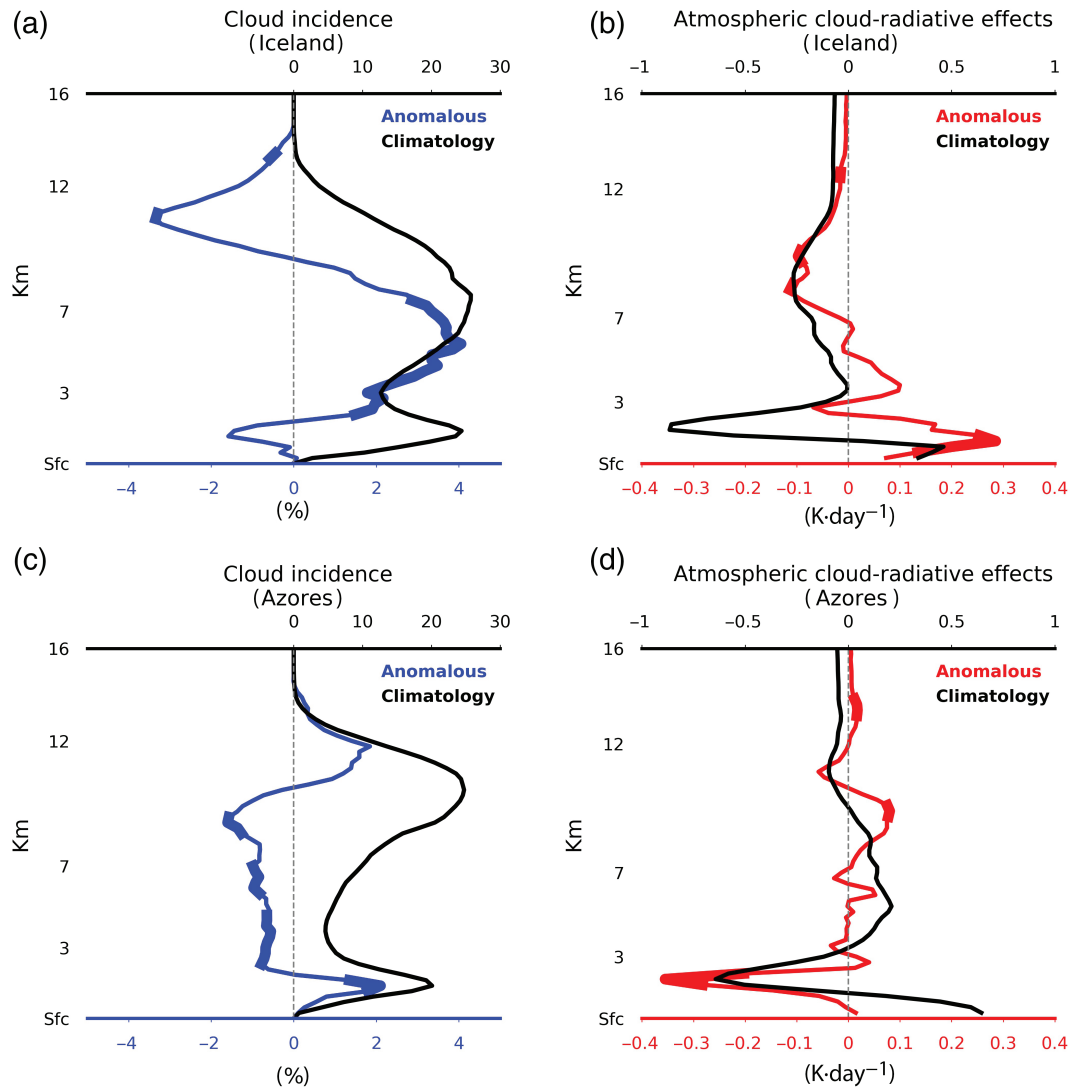


FIGURE 3 Vertical profiles of NAO regressions of DJF 5-day mean (a, c) cloud incidence (blue) and (b, d) ACRE (red) averaged over the (a, b) Iceland and (c, d) Azores domains. The black lines indicate the DJF climatology during 2006–2011. Thick lines denote statistical significance at the 5% level according to a two-sided Wald test

and an upward shift of the climatological low-level maximum of cloud incidence. In the upper troposphere, the downward shift of high-level cloud tops and the increased mid-level cloud incidence lead to anomalous ACRE cooling. In the lower troposphere, the decrease in low-level cloud incidence leads to anomalous ACRE heating.

3.3.2 | Azores

Over the Azores domain, the vertical profile of climatological cloud incidence exhibits two maxima: an upper-level maximum at 10 km and a low-level maximum at 1.5 km (Figure 3c; black). This leads to climatological ACRE cooling near the high-level and low-level cloud tops, and ACRE heating between in the mid-troposphere and near

the surface underneath the low-level clouds (Figure 3d; black).

As for the Iceland domain, the impact of the NAO is on the order of 20% of the climatological value for cloud incidence (Figure 3c, blue) and up to 50% for ACRE (Figure 3d, red). The NAO impact is opposite to that over the Iceland domain. During a positive phase of the NAO, cloud incidence increases around 12 km and around 1.5 km, and decreases between. This indicates an upward shift of high-level clouds, consistent with a rising tropopause, and an increase in low-level clouds, consistent with enhanced large-scale descent and enhanced low-level stability. As a result, a positive phase of the NAO is associated with anomalous ACRE heating in the upper troposphere and increased ACRE cooling in the lower troposphere. These ACRE changes are opposite to those over the Iceland domain.

3.4 | Robustness in other observational datasets

We now verify that the NAO impact on vertically integrated ACRE averaged over the Iceland and Azores domains is robust in sign with respect to the choice of the observational dataset. To this end we compare the CloudSat/CALIPSO results to CERES-SYN1deg, CERES-EBAF and GERB/SEVIRI (Table 1).

Because GERB/SEVIRI is only available for the long-wave component, the comparison is restricted to that for all datasets. This is unproblematic, since ACRE is dominated by this component anyway (Figure 1b). CERES-EBAF and GERB/SEVIRI are available only on the monthly time-scale. The comparison between the 5-day means from CloudSat/CALIPSO and CERES-SYN1deg and the monthly means from CERES-EBAF and GERB/SEVIRI indicates to what extent the NAO impact is sensitive to the averaging period.

The CRE anomalies at the TOA and BOA differ between the datasets by several $W \cdot m^{-2}$ and are not always statistically significant. Nevertheless, the vertically integrated ACRE anomalies, which are computed from the difference of TOA and BOA anomalies, are more robust and agree on the sign. All datasets show vertically integrated ACRE cooling over the Azores domain during a positive NAO phase, and heating over the Iceland domain. This robustness in sign supports the results of the CloudSat/CALIPSO analysis, although the comparison also illustrates the uncertainty in the magnitude of the NAO impact on ACRE. The comparison between ACRE changes derived from the 5-day means from CloudSat/CALIPSO and CERES-SYN1deg and the monthly means

from CERES-EBAF and GERB/SEVIRI shows that the uncertainty in the magnitude of the NAO impact does not primarily arise from the averaging period. We will study the importance of these heating/cooling anomalies for the dynamics of the NAO in the next section.

4 | ROLE OF ACRE FOR THE DYNAMICS OF THE NAO: ERA-INTERIM ANALYSIS

In the previous section we found that a positive NAO leads to anomalous ACRE cooling over the Azores high and ACRE heating over the Iceland low. This heating pattern could alter atmospheric temperatures, air density, surface pressure and hence the NAO. More specifically, the heating pattern suggests the possibility of a positive cloud-radiative feedback that amplifies the sea-level pressure contrast between the Azores and Iceland and increases the NAO persistence. This is opposite to the negative cloud-radiative feedback suggested by Li *et al.* (2014a).

To study the role of ACRE for the NAO dynamics, we apply the surface pressure tendency equation (PTE) of Knippertz and Fink (2008) and Fink *et al.* (2012) using ERA-Interim data. Before detailing the PTE analysis, we first confirm that ERA-Interim captures the observed NAO impact on clouds and ACRE.

Figure 4 shows the impact of the NAO on high-level, mid-level and low-level cloud cover in ERA-Interim for DJF from 1979 to 2017 by means of 5-day mean regressions. In ERA-Interim, sigma levels are used to distinguish high-level, mid-level and low-level cloud cover (ECMWF,

TABLE 1 NAO impact on long-wave vertically integrated ACRE as well as TOA and BOA cloud-radiative effects during December–February over the Iceland and Azores domains in satellite datasets and ERA-Interim

	CERES-SYN1deg (2000–2017)	CloudSat/CALIPSO (2006–2011)	CERES-EBAF (2002–2017)	GERB/SEVIRI (2006–2011)	ERA-Interim (1979–2017)
<i>Iceland</i>					
TOA	+2.7(±0.7)	+3.2(±1.0)	+2.1(±0.9)	+1.9(±1.0)	+2.1(±0.9)
ACRE	+1.9(±0.9)	+1.0(±0.7)	+2.1(±1.2)	+1.7(±1.1)	+4.0(±0.5)
BOA	+0.8(±0.5)	+2.2(±0.9)	0.0(±0.8)	+0.2(±0.7)	−1.9(±0.8)
<i>Azores</i>					
TOA	−2.2(±0.7)	−0.1(±1.5)	−2.3(±1.2)	−1.5(±0.9)	−2.1(±0.7)
ACRE	−2.5(±0.8)	−1.5(±0.8)	−2.4(±1.1)	−0.7(±0.5)	−2.5(±0.5)
BOA	+0.3(±0.4)	+1.4(±1.5)	+0.1(±0.6)	−0.8(±0.5)	+0.4(±0.8)

Note: For CloudSat/CALIPSO, CERES-SYN1deg and ERA-Interim, 5-day means are used. For CERES-EBAF and GERB/SEVIRI monthly means are used. The analyzed time periods are given in parentheses. Bold numbers indicate statistical significance at the 5% level according to a two-sided Wald test, with the confidence interval given in parentheses.

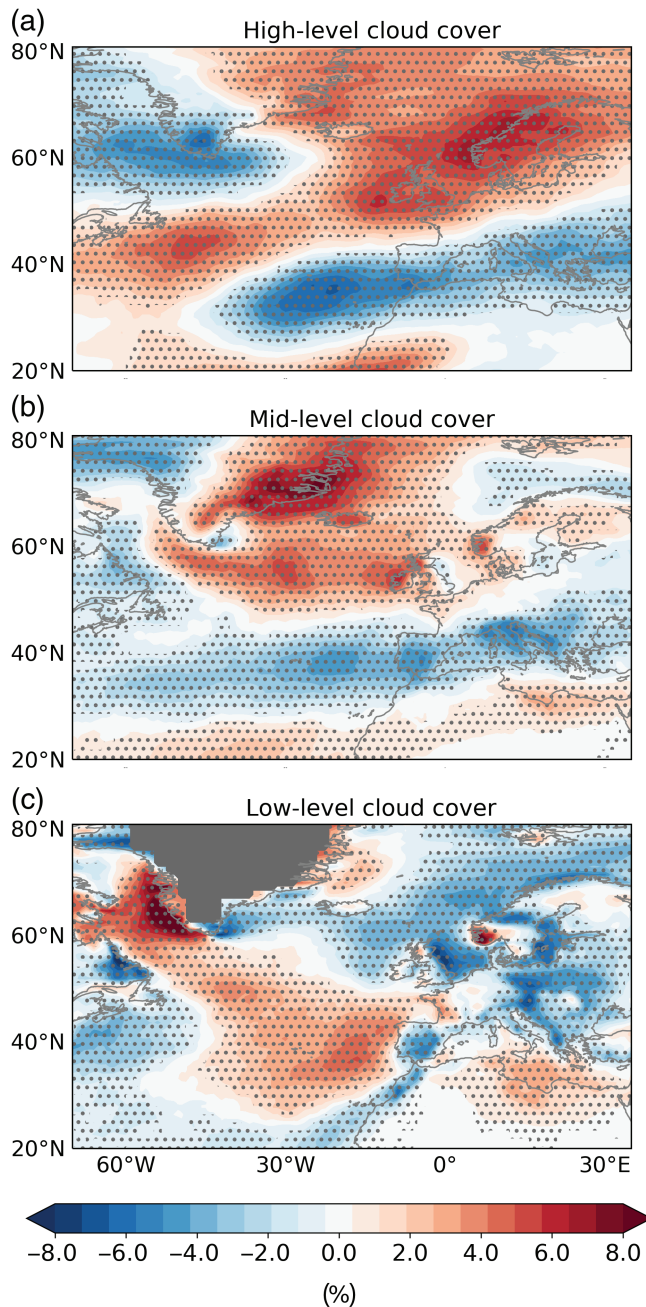


FIGURE 4 NAO regressions of DJF 5-day mean ERA-Interim (a) high-level, (b) mid-level and (c) low-level cloud cover during 1979–2017. The boundary between the mid- and high-level clouds is at 450 hPa, and the boundary between mid- and low-level clouds is at 800 hPa. Stippling indicates statistical significance at the 5% level according to a two-sided Wald test. For (c), Greenland is masked out

2010), with boundaries at roughly 800 and 450 hPa. Figure 4a illustrates that a positive NAO is associated with increased high-level cloud cover along the storm track (near 45°N), the subpolar North Atlantic, and Scandinavia. Mid-level cloud anomalies (Figure 4b) exhibit a meridional dipole structure with positive anomalies poleward of the storm track and east of Greenland, and negative anomalies

equatorward of the storm track. The anomalies in low-level cloud cover are largely opposite to those of high-level cloud cover (Figure 4c). These results are qualitatively consistent with CloudSat/CALIPSO (Figure 2), apart from near Iceland and over the Norwegian Sea. These discrepancies might partly result from the fact that ERA-Interim measures cloud cover and CloudSat/CALIPSO cloud incidence, which leads to different treatments of cloud overlap in the two datasets (Section 2).

More importantly, and more relevant to the NAO dynamics, the regression analysis of 5-day mean vertically integrated ACRE during DJF from 1979–2017 and 2006–2011 in Figure 5a,b shows an ACRE dipole that is broadly consistent with the satellite observations (Figure 2d–f), albeit weaker. An exception is the Labrador Sea. The vertical profiles of the climatological ACRE and the NAO-generated ACRE anomalies over the Iceland and Azores domains (Figure 5c,d) show a similar structure as in CloudSat/CALIPSO (Figure 3b,d). In ERA-Interim the heating anomalies are statistically significant at almost all levels and smoother, while the maxima of the regressions are slightly weaker over the Azores and slightly stronger over Iceland than CloudSat/CALIPSO. For vertically averaged ACRE, ERA-Interim is qualitatively consistent with the observations (Table 1). Thus, we conclude that ERA-Interim overall captures the observed impact of the NAO on clouds and ACRE.

4.1 | Surface pressure tendency equation (PTE)

The PTE allows us to quantify the impact of heating and moisture anomalies on the surface pressure evolution. We use the PTE to assess the relative importance of NAO-generated ACRE changes with respect to changes in other diabatic processes, such as latent heating and clear-sky radiation, and changes in temperature advection by the circulation. The PTE is given by

$$\underbrace{\frac{\partial p_{\text{sfc}}}{\partial t}}_{Dp} = \underbrace{\rho_{\text{sfc}} \frac{\partial \phi_{100 \text{ hPa}}}{\partial t}}_{D\phi} + \underbrace{\rho_{\text{sfc}} R_d \int_{\text{sfc}}^{100 \text{ hPa}} \frac{\partial T_v}{\partial t} d(\ln p)}_{\text{ITT}} + \underbrace{g(E - P)}_{E-P} + \text{RES}_{\text{PTE}}, \quad (3)$$

where p_{sfc} is the surface pressure, p is air pressure, ρ_{sfc} is the surface air density, R_d is the gas constant of dry air, $\phi_{100 \text{ hPa}}$ is the geopotential at 100 hPa, T_v is the virtual temperature, g is the gravitational acceleration, E is evaporation, P is precipitation, and RES_{PTE} represents the analysis residual due to, for example, spatiotemporal discretisation. Equation (3) measures the surface pressure

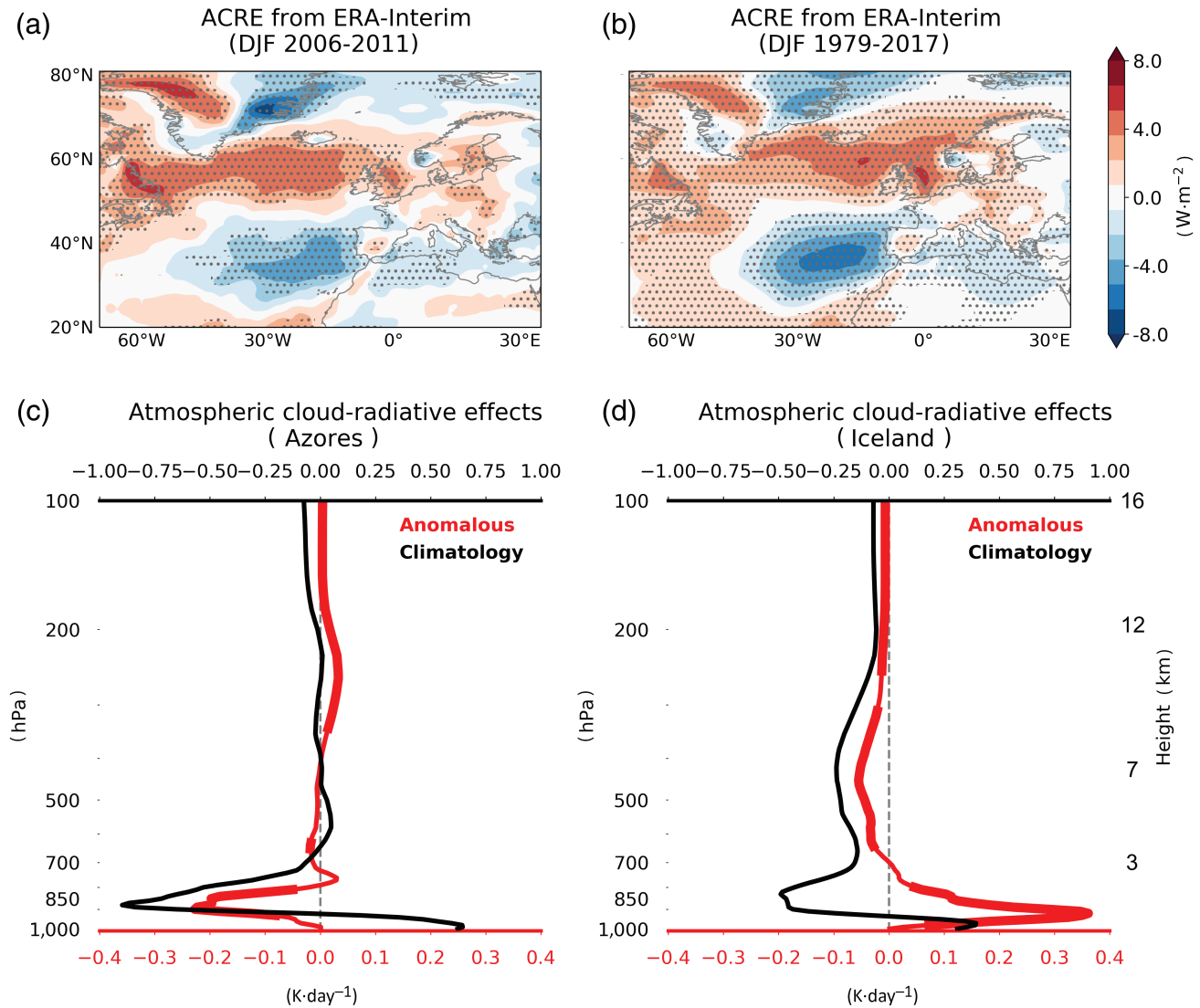


FIGURE 5 NAO regression of DJF 5-day mean ACRE in ERA-Interim; vertically integrated ACRE during (a) 2006–2011 and (b) 1979–2017. Vertical profiles of ACRE regression during 2006–2011 averaged over the (c) Azores and (d) Iceland domains. The black lines indicate the DJF climatology during 2006–2011. Stippling in (a, b) and thick lines in (c, d) indicate statistical significance at the 5% level according to a two-sided Wald test

tendency (Dp) from changes in the upper boundary of the vertical integral, here chosen as the geopotential at 100 hPa level ($D\phi$), changes in virtual temperature between this boundary and the surface (ITT), and changes in column mass due to evaporation and precipitation (E–P).

Because we are interested in clouds, we focus on the ITT term, which we decompose further into

$$ITT = \rho_{\text{sfc}} R_d \int_{\text{sfc}}^{100 \text{ hPa}} -\mathbf{v} \cdot \nabla_p T_v d(\ln p) \quad \text{TADV} \quad (4a)$$

$$+ \rho_{\text{sfc}} R_d \int_{\text{sfc}}^{100 \text{ hPa}} \left(\frac{R_d T_v}{c_p p} - \frac{\partial T_v}{\partial p} \right) \omega d(\ln p) \quad \text{VMT} \quad (4b)$$

$$+ \rho_{\text{sfc}} R_d \int_{\text{sfc}}^{100 \text{ hPa}} \frac{T_v Q}{c_p T} d(\ln p) \quad \text{PHY} \quad (4c)$$

$$+ \rho_{\text{sfc}} R_d \int_{\text{sfc}}^{100 \text{ hPa}} 0.608 T \frac{dq}{dt} d(\ln p) \quad \text{HUM} \quad (4d)$$

$$+ RES_{ITT}, \quad (4e)$$

where \mathbf{v} is the horizontal wind, ω is the pressure velocity, c_p is the specific heat capacity at constant pressure, T is the air temperature, Q is the total temperature tendency from subgrid-scale diabatic processes, q is the specific humidity, and RES_{ITT} is the analysis residual. Thus, the ITT term is decomposed into contributions from horizontal temperature advection (TADV), vertical motions (VMT) and diabatic processes (PHY+HUM). PHY measures the impact of diabatic processes on temperature, e.g., latent heat release due to phase changes of water, radiative

heating, sensible heat fluxes and boundary-layer turbulence, whereas HUM measures the impact of diabatic processes on the amount of specific humidity (e.g., a specific humidity decrease due to condensation of water vapour). In the following, the sum of PHY and HUM is referred to as the total diabatics term DIAB. The DIAB term contains the all-sky radiative heating, which we further separate below into contributions from ACRE and clear-sky radiative heating.

The PTE is a budget equation of the surface pressure tendency. Given a constant upper boundary in geopotential height ($D\phi = 0$), a process that warms the atmosphere between the surface and the upper boundary leads to decreased air density, mass loss and surface pressure fall. Analogously, a process that cools the atmosphere works in favour of a surface pressure rise. A detailed description of the PTE analysis is given in Fink *et al.* (2012). We chose the upper boundary at 100 hPa, following Fink *et al.* (2012). The choice of the upper boundary can affect the relative contributions of ITT and $D\phi$ (Knippertz *et al.*, 2009). Because clouds are limited to the troposphere, the 100 hPa boundary ensures that the cloud-radiative impact is captured as part of the ITT term. We note that the vertical integrals are performed over $d(\ln p)$ (and not dp), so that a heating in the upper troposphere has a stronger impact on the surface pressure tendency than a heating in the lower troposphere. As we will see below for the ACRE impact over Iceland, this can lead to a zero surface pressure tendency impact despite a vertically integrated anomalous ACRE heating.

We calculate the PTE and its decomposition every 6 hr over the entire North Atlantic region, and then construct 5-day means. Figure 6a illustrates the 5-day mean PTE terms for the Iceland domain during DJF 2006/2007. Generally speaking, both the ITT and $D\phi$ terms are substantial and often compensate each other. Note that the instantaneous correlation between the Dp term and the NAO index is not statistically significant. However when Dp leads the NAO by a 5-day mean period, there is a weak but statistically significant negative correlation. The decomposition of the ITT term (Figure 6b) shows large and opposite contributions from horizontal temperature advection (TADV) and vertical motions (VMT). TADV and VMT tend to be negatively correlated because a column-mean warming from horizontal temperature advection ($TADV > 0$) is associated with upward motions and adiabatic cooling ($VMT < 0$), and *viceversa*. In the following, we will therefore consider the sum $DYN = TADV + VMT$ to measure the surface pressure impact of the circulation. The contributions from the sum of all diabatic processes (DIAB) and ACRE are smaller than TADV and VMT, but they can still considerably affect the ITT term because of the compensation between TADV and VMT.

As for the analysis of the NAO impact on clouds in Section 3, we regress the 5-day means of the PTE terms onto the NAO index. In particular, the diabatic heating terms in the PTE are not directly constrained by observations and therefore depend to some extent on the model parametrizations of ERA-Interim. Yet, the NAO-generated anomalies in vertically integrated ACRE over the Azores and Iceland domains derived from ERA-Interim are qualitatively consistent with the observations (Table 1). Moreover, Ling and Zhang (2013) showed that ERA-Interim's diabatic heating profiles in the extratropics compare well with other reanalysis datasets and observations. This indicates that our PTE results should not be overly sensitive to the choice of the reanalysis dataset.

4.2 | Latitude–longitude perspective of the PTE regression analysis

We start with the latitude–longitude perspective of the NAO regression of the PTE terms (Figure 7). A positive NAO is associated with a positive surface pressure tendency in a region that extends from Iceland over the North Sea to the Iberian Peninsula, as well as over western parts of the North Atlantic west of the Azores. A negative surface pressure tendency is found over the Labrador Sea and the Irminger Sea. The surface pressure tendency pattern results from large and opposite tendencies of the $D\phi$ and ITT terms. The $D\phi$ term dominates over western Europe and over the Labrador Sea and the Irminger Sea (Figure 7b). The ITT term dominates over the northeastern and the western parts of the North Atlantic (Figure 7c). A positive NAO is associated with a weakening of the Iceland low due to changes in virtual temperature changes between 100 hPa and the surface (i.e., the ITT term), and a strengthening of the western and eastern edges of the Azores high. This is consistent with a beginning decay of the positive phase of the NAO.

We now decompose the ITT anomalies into the contributions of Equation (4) so as to assess their relative importance for the NAO dynamics, with the horizontal advection term TADV and the vertical motions term VMT shown as the sum $DYN = TADV + VMT$ (Figure 8; note the different magnitudes of each term). The ITT anomalies result from meridional dipoles in DYN and DIAB, which largely oppose each other. The large-scale dynamics (DYN) work in favour of dampening the NAO surface pressure anomalies (shown in black, Figure 8b), while diabatic processes as a whole (DIAB) work in favour of reinforcing them (Figure 8c). The magnitude of the DIAB anomalies is almost as large as the DYN anomalies, and in fact larger west of the Azores. The meridional dipole of the DIAB anomalies suggests that diabatic processes as

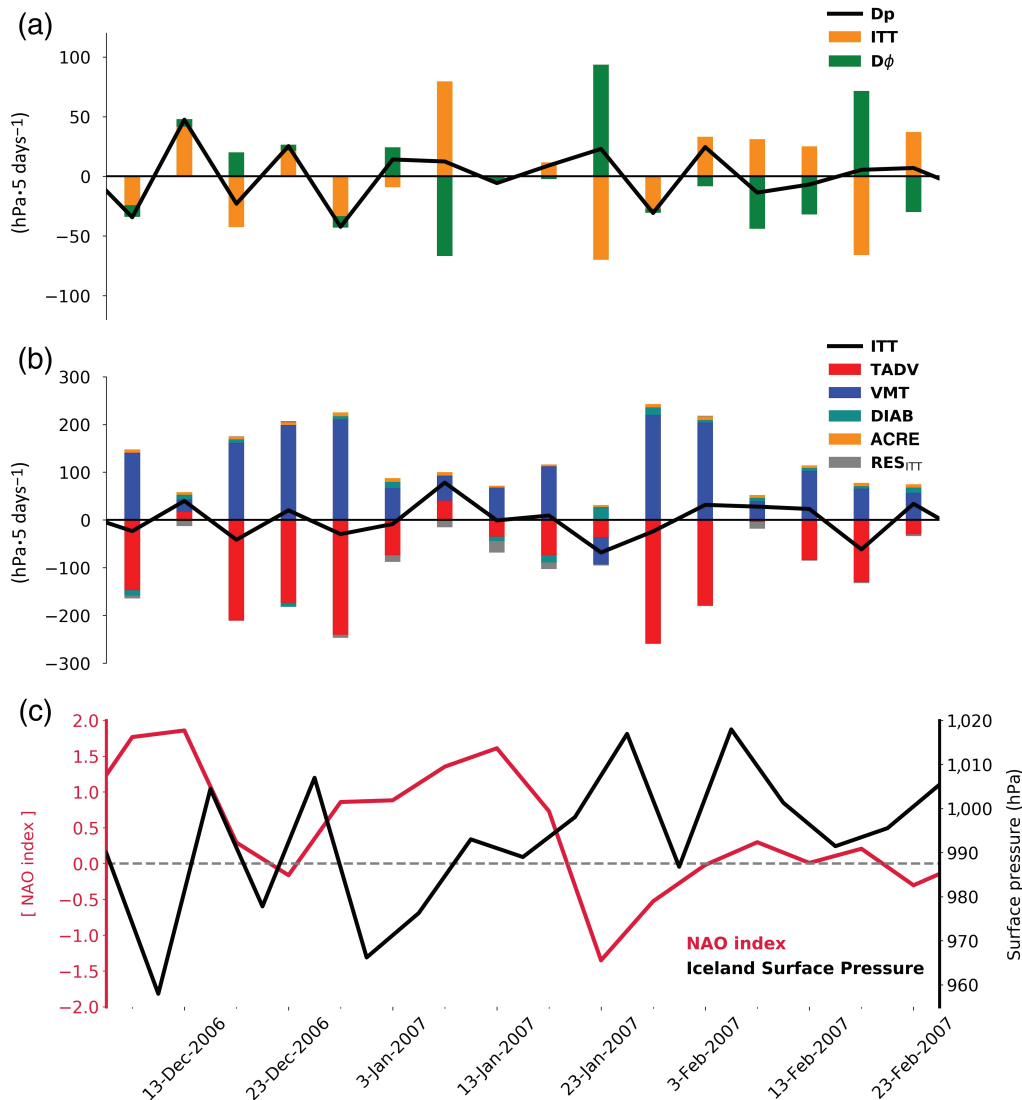


FIGURE 6 Illustration of the pressure tendency equation (PTE) analysis using ERA-Interim data over the Iceland domain during DJF 2006/2007. (a) Surface pressure tendency and decomposition. (b) Decomposition of the ITT term. (c) NAO index and area-average surface pressure. Note that the instantaneous surface pressure is shown for the beginning of each 5-day period. The E-P and RES_{PTE} are near zero and not included here. Section 4 gives a detailed explanation of the PTE terms

a whole positively feed back on the NAO by reinforcing both the Iceland low and the Azores high during a positive NAO phase. ERA-Interim does not allow us to quantify the individual contribution of latent heating. However by analysing precipitation anomalies associated with the NAO, we can approximate its spatial distribution. Figure 9 illustrates that a positive phase of the NAO is associated with strong positive anomalies of 5-day mean precipitation in the higher midlatitudes and strong negative anomalies in lower midlatitudes. The spatial correspondence of the diabatic anomalies with the NAO-generated precipitation anomalies indicates that latent heating is the dominant process, in line with Greatbatch and Jung (2007) and Woollings *et al.* (2016).

The DIAB anomalies contain the sum of all diabatic processes. To assess the role of ACRE and clear-sky

radiative heating, we also regress surface pressure tendencies due to ACRE (Figure 8d) and clear-sky radiative heating (Figure 8e) onto the NAO. A positive NAO is associated with positive surface pressure tendency anomalies due to ACRE around the Azores, consistent with anomalous vertically integrated ACRE cooling (Figure 5). Around Iceland, the pattern is less consistent, with negative surface pressure tendency anomalies south of Iceland and positive anomalies north of Iceland. Averaged over the Azores and Iceland domains, during a positive NAO phase the ACRE anomalies slightly reinforce the Azores high but have no impact on the strength of the Iceland low (Table 2). The PTE regressions thus indicate that the ACRE anomalies, via strengthening the Azores high, are a small positive feedback on the NAO and its persistence. Similarly, the anomalies from clear-sky

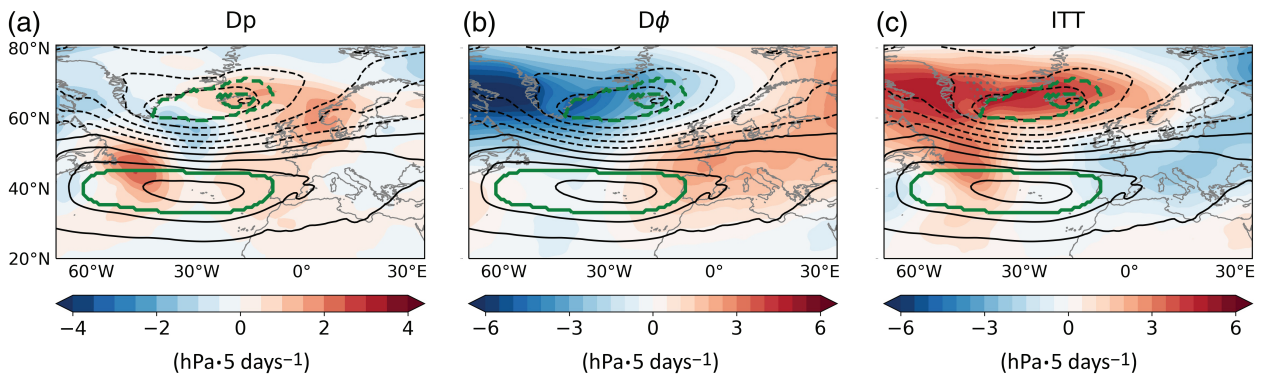


FIGURE 7 NAO regressions of 5-day mean (a) surface pressure tendency and contributions from tendencies of (b) the 100 hPa geopotential height and (c) the virtual temperature. Black lines show the NAO-related surface pressure anomaly (contour interval 2 hPa; dashed lines indicate negative anomalies). The green lines indicate the Azores and Iceland regions according to Figure S1. For the Iceland domain land is excluded, as indicated by the inner green dashed line. Results are based on DJF ERA-Interim data from 2006–2011. Note the different colour scales

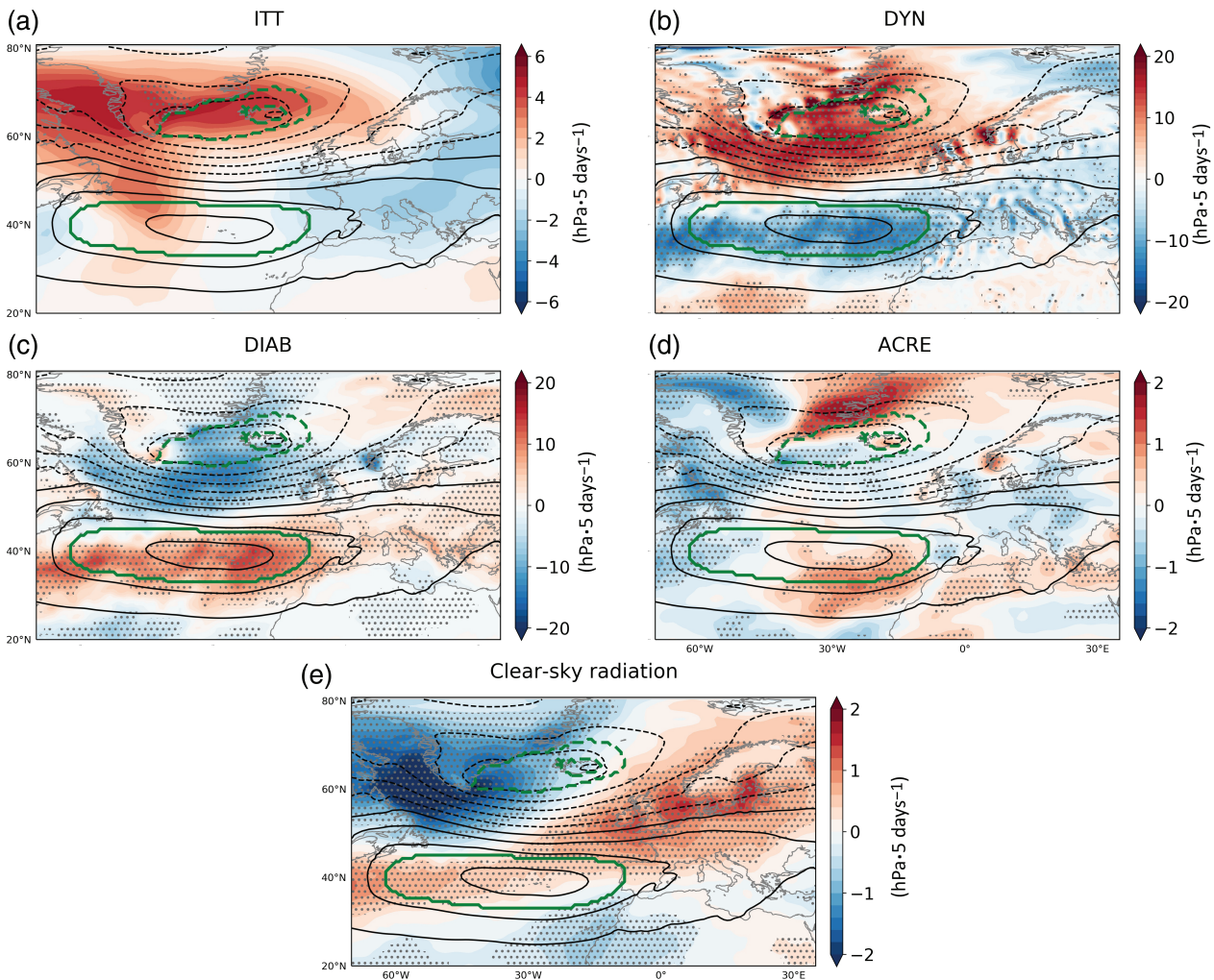


FIGURE 8 NAO regressions of 5-day mean surface pressure tendencies from (a) changes in virtual temperature (ITT), (b) large-scale dynamics (DYN), (c) diabatic processes (DIAB), (d) atmospheric cloud-radiative effects (ACRE) and (e) clear-sky radiation. Results are based on ERA-Interim data during DJF from 2006 to 2011. Black lines show the NAO-related surface pressure anomaly (contour interval 2 hPa; dashed lines indicate negative anomalies). Stippling indicates statistical significance at the 5% level according to a two-sided Wald test. Note the different colour scales. The green lines indicate the Azores and Iceland regions according to Figure S1. For the Iceland domain, land is excluded, as indicated by the inner green dashed line

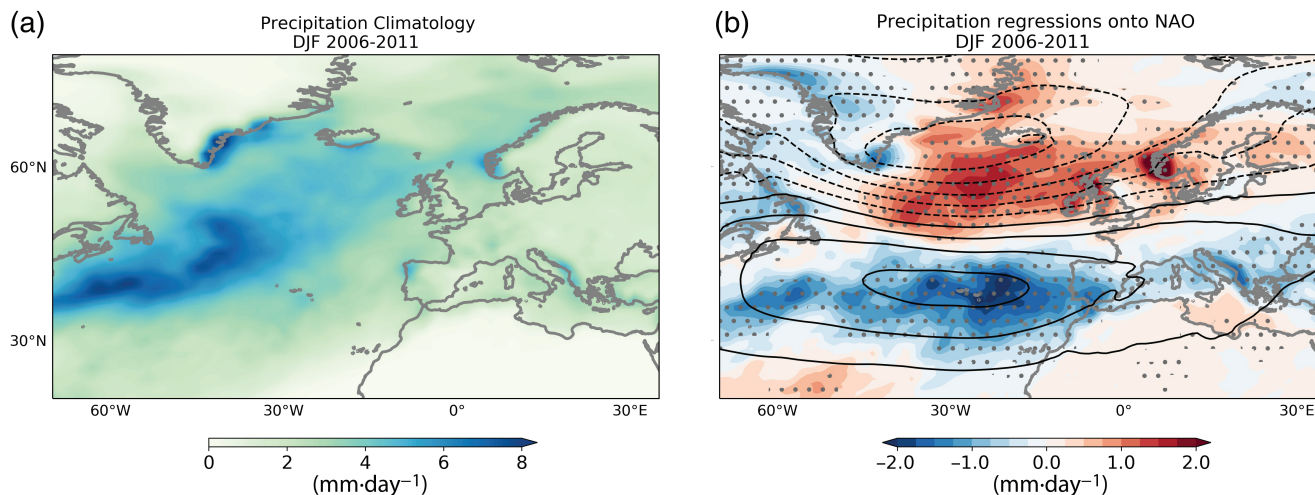


FIGURE 9 ERA-Interim DJF precipitation from 2006–2011; (a) climatology, (b) NAO regressions of 5-day means with stippling indicating statistical significance at the 5% level according to a two-sided Wald test and black lines showing the NAO-related surface pressure anomaly (contour interval 2 hPa; dashed lines indicate negative anomalies)

radiative heating act as a positive feedback by reinforcing both the Iceland low and Azores high. The clear-sky radiative heating impact over the Azores is associated with anomalous column-mean heating (Figure S2) which leads to anomalous column-mean clear-sky radiative cooling, while the opposite occurs over Iceland. Yet, the contribution of ACRE and clear-sky radiative heating to the diabatic processes as a whole is relatively minor, suggesting that radiative feedbacks on the NAO are small (Table 2).

4.3 | Vertical perspective on the PTE regression analysis over Iceland and the Azores

To better understand the impact of the ITT term and its decomposition, we study the vertical profiles of the regressions averaged over the Iceland and Azores domains. This is shown in Figure 10.

TABLE 2 NAO regressions of 5-day mean surface pressure tendencies from different contributions to the ITT term

	Azores	Iceland
DYN	-9.6(±2.9)	+11.5(±5.8)
DIAB	+8.5(±2.2)	-7.0(±2.2)
ACRE	+0.2(±0.2)	0.0(±0.3)
Clear-sky radiation	+0.4(±0.2)	-0.8(±0.5)

Note: Values are vertically integrated and averaged over the Azores and Iceland domains. The analysis is based on ERA-Interim during DJF from 2006 to 2011. Bold numbers indicate statistical significance at the 5% level according to a two-sided Wald test, with the confidence interval given in parentheses.

Over the Azores domain (Figure 10a), a positive NAO is associated with large negative tropospheric DYN anomalies between the surface and 300 hPa, which are opposed by large positive DIAB anomalies. In the upper troposphere, the DIAB contribution is slightly positive due to a positive anomaly from clear-sky radiation, with a small negative ACRE anomaly. Near the surface, i.e. from 950 to 800 hPa, roughly 20–30% of the DIAB anomalies are caused by ACRE, but otherwise the ACRE anomalies are near zero. Overall, the surface pressure tendency anomaly over the Azores domain is positive during a positive NAO phase due to diabatic processes unrelated to radiation.

A very similar but opposite picture of anomalies occurs over the Iceland domain (Figure 10b).

5 | COMPARISON TO LI ET AL. (2014A)

Our work is motivated by Li *et al.* (2014a). In contrast to our conclusion of a weak positive cloud-radiative feedback on the NAO, Li *et al.* (2014a) argued for a negative feedback (although they did not quantify the magnitude of the feedback). To understand this difference, this section contrasts our analysis method and interpretative framework with that of Li *et al.* (2014a).

The main differences are the analysis of CRE within the atmosphere (ACRE) instead of TOA CRE, the use of 5-day means instead of monthly means, the use of the NAO instead of the AO index, and the study of the winter months of December–January–February instead of the extended winter from October to March.

These differences lead to substantial deviations in the zonal-mean anomalies of CloudSat/CALIPSO cloud

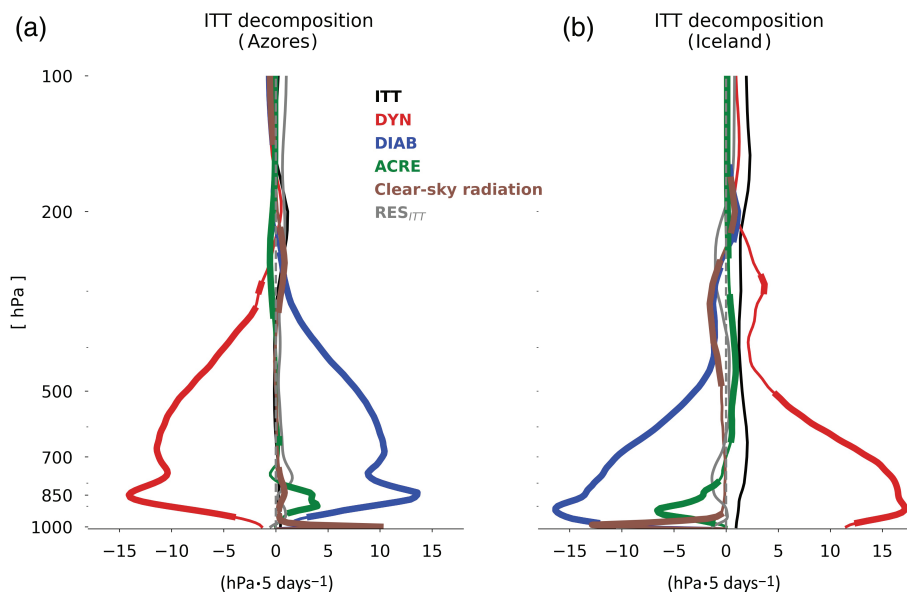


FIGURE 10 NAO regressions of 5-day mean vertical profiles of the ITT term and its decomposition over the (a) Azores and (b) Iceland domains. Results are based on ERA-Interim data during DJF from 2006 to 2011. Thick lines indicate statistical significance at the 5% level according to a two-sided Wald test

incidence (Figure 11), consistent with Li and Thompson (2016). However, apart from the zonal-mean cloud incidence, our regression results are very similar to those of Li *et al.* (2014a). This includes the zonal-mean CRE regression (compare our Figure 1b with figure 2e of Li *et al.*, 2014a) as well as the North Atlantic regressions for clouds and CRE (compare our Figures 2a, 4a and 5a to figures 3b, 3c and 4c from Li *et al.*, 2014a). Moreover, Table 2 indicates that the ACRE and TOA CRE anomalies closely resemble each other, at least when averaged over the Azores and Iceland domains. Thus, the difference in the concluded direction of the cloud-radiative feedback on the NAO does not result from differences in the analysis method, but from different interpretative frameworks.

Li *et al.* (2014a) applied a temperature anomaly framework. Looking down from the TOA, they found negative CRE anomalies (i.e., cooling) around the Azores during a positive NAO, while tropospheric temperatures are anomalously warm (as inferred from TOA clear-sky long-wave radiation). Li *et al.* (2014a) interpreted this as a cloud-radiative dampening of NAO-generated temperature anomalies and hence a negative cloud-radiative feedback. Yet, their framework ignores the vertical pattern of temperature and CRE anomalies. A comparison between Figure 5c,d with Figure S2 shows that the CRE anomalies do not follow the vertical profile of the temperature anomalies and are strongest in the lower troposphere where the temperature anomalies are weakest. In our view, the mismatch in vertical location questions the picture of a cloud-radiative dampening of temperature anomalies and hence Li *et al.*'s (2014a) conclusion of a negative cloud-radiative feedback.

We instead apply a surface pressure tendency framework, where the vertically integrated effect of CRE

matters but not the vertical location of CRE with respect to temperature anomalies. In this perspective, the vertically integrated negative ACRE anomalies over the Azores during a positive NAO strengthen the high and so act as a positive cloud-radiative feedback. We believe that this framework is better suited to infer the cloud-radiative feedback, as it circumvents potential problems from the vertical mismatch of temperature and CRE anomalies. However, model simulations would be needed to test this observationally based result.

6 | CONCLUSIONS

The North Atlantic Oscillation is a dominant mode of synoptic-scale variability over the North Atlantic region. In this paper, we have studied (a) how NAO variability on synoptic time-scales affects clouds and cloud-radiative effects (CRE), and (b) the potential of these NAO-generated changes in CRE to in turn affect the NAO. Our work was motivated by the hypothesis of Li *et al.* (2014a) that TOA CRE act as a negative feedback on the NAO and dampens NAO variability. Our work is the first to study the NAO-CRE coupling on synoptic time-scales, and to quantify its importance relative to large-scale dynamics and diabatic processes as a whole. Since we are interested in synoptic time-scales, we are specifically considering the role of CRE within the atmosphere (ACRE).

The NAO has robust impacts on clouds and ACRE in a range of satellite observations and ERA-Interim short-term forecasts. A positive phase of the NAO is associated with more high-level clouds along the storm track (45°N) and the subpolar Atlantic, and less high-level clouds poleward and equatorward of it. The high-level

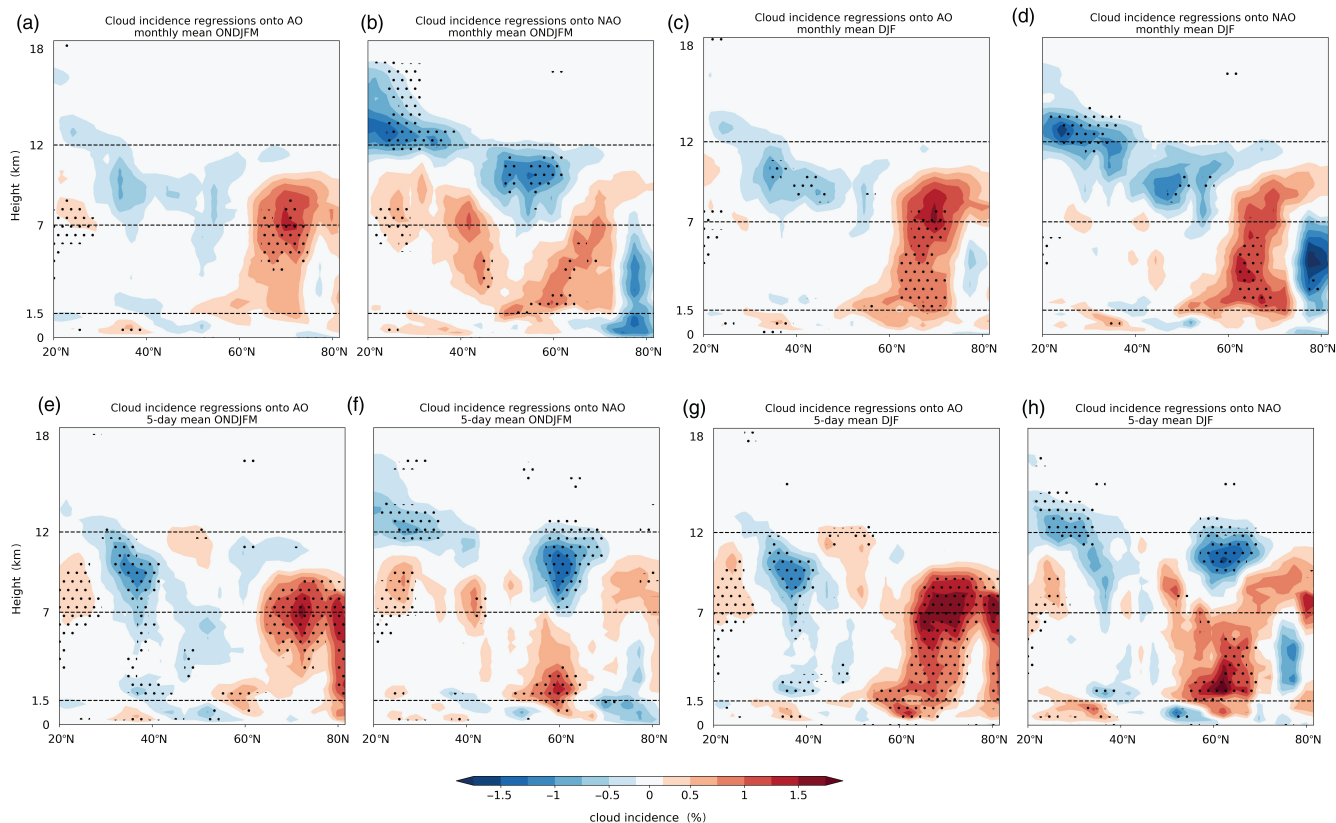


FIGURE 11 Regression of zonal-mean cloud incidence from CloudSat/CALIPSO onto the (a, c, e, g) AO and (b, d, f, h) NAO for (a–d) monthly means and (e–h) 5-day means, and for (c, d, g, h) DJF and (a, b, e, f) ONDJFM. (a) corresponds to Li *et al.* (2014a), (h) corresponds to our study. The other panels indicate the impact of changing the circulation index, the averaging period, and the number of months considered. Stippling indicates statistical significance at the 5% level according to a two-sided Wald test

cloud changes are consistent with stronger upward motion and a lowered tropopause. For low-level clouds, the NAO impact is opposite to that of high-level clouds, with more low-level clouds around the Azores, consistent with stronger descending motion, and less low-level clouds around and south of Iceland. The NAO-associated cloud changes lead to a dipole of anomalous vertically integrated ACRE cooling over the Azores and heating over Iceland that is robust in sign (but not in magnitude) across satellite datasets and the ERA-Interim short-term forecasts.

To study to what extent the ACRE anomalies in turn affect the NAO and its persistence, we apply the surface pressure tendency equation (PTE) to ERA-Interim short-term forecast data. This allows us to quantify the relative role of ACRE compared to the large-scale circulation and the sum of all diabatic processes. The regression analysis indicates that the NAO-generated ACRE anomalies over the Azores feed back positively on the NAO and so should increase its persistence. This result is in contrast to Li *et al.* (2014a), who suggested that TOA CRE should decrease the NAO persistence. As discussed in Section 5, we believe the difference between our study and theirs lies in the interpretative framework. While we consider the

surface pressure tendency, Li *et al.* (2014a) reason based on a CRE dampening of NAO-generated temperature anomalies. Irrespective of this difference in the concluded direction of the cloud-radiative impact, our analysis also shows that the cloud-radiative impact is minor compared to the impact of diabatic processes as a whole. This suggests that cloud-radiative effects are not crucial to the NAO dynamics on synoptic time-scales.

Diabatic processes as a whole, which besides CRE include latent heating, exhibit NAO-generated changes that strongly project onto the NAO surface pressure anomalies. The changes in diabatic processes appear to be dominated by latent heating, consistent with previous work (Greatbatch and Jung, 2007; Woollings *et al.*, 2016). Our PTE analysis indicates that diabatic processes as a whole constitute a substantial positive feedback on the NAO. This is consistent with Woollings *et al.* (2016) who show that latent heating shifts with the jet stream and balances the adiabatic destruction of baroclinicity by the circulation. However, our result is in contradiction to the modelling work of Greatbatch and Jung (2007) and Xia and Chang (2014), who argue that latent heating acts as a negative feedback and dampens the persistence of the

NAO and the annular modes, respectively. As for CRE, we believe the difference results from the chosen interpretative framework. Greatbatch and Jung (2007) and Xia and Chang (2014) argue with a dampening of NAO-generated temperature anomalies, whereas we reason based on the surface pressure tendency.

In summary, we have documented robust impacts of the NAO on clouds and cloud-radiative effects over the North Atlantic and the neighbouring regions. Our analysis suggests that cloud-radiative effects represent a positive but small feedback on the NAO persistence on synoptic time-scales. In the future we plan to test our PTE-based hypothesis by means of atmospheric model simulations. This will also allow us to clarify the differences between interpretative frameworks, and to investigate in more detail the role of diabatic processes.

ACKNOWLEDGEMENTS

We thank the two anonymous reviewers for their thoughtful reviews and suggestions that improved the quality of the manuscript. GP and AV are supported by the German Ministry of Education and Research (BMBF) and Research for Sustainable Development (FONA): (<http://www.fona.de>) under grant agreement 01LK1509A. This work contributes to the project HD(CP)²: High-Definition Clouds and Precipitation for advancing Climate Prediction and to subproject C5 "Forecast uncertainty for peak surface gusts associated with European cold-season cyclones" of the Transregional Collaborative Research Centre SFB/TRR 165 "Waves to Weather", funded by the German Research Foundation (DFG). The CloudSat/CALIPSO data were obtained from the CloudSat Data Processing Center (<http://www.cloudsat.cira.colostate.edu>). Ying Li is thanked for providing an insolation routine, which was helpful to compute short-wave heating rates from CloudSat/CALIPSO. The ERA-Interim reanalysis data were obtained from the ECMWF Mars archive. For the Wald test, the SciPy library was used (<https://www.scipy.org>). For the postprocessing of the satellite and reanalysis data, the Climate Data Operator (CDO) software was used (<https://code.mpimet.mpg.de/projects/cdo/>). (all sites accessed 24 February 2020)

ORCID

Georgios Papavasileiou  <https://orcid.org/0000-0002-8544-4123>

Aiko Voigt  <https://orcid.org/0000-0002-7394-8252>

Peter Knippertz  <https://orcid.org/0000-0001-9856-619X>

REFERENCES

Albern, N., Voigt, A. and Pinto, J.G. (2019) Cloud-radiative impact on the regional responses of the midlatitude jet streams and storm

tracks to global warming. *Journal of Advances in Modeling Earth Systems*, 11(7), 1940–1958.

Ambaum, M.H.P. and Hoskins, B.J. (2002) The NAO troposphere-stratosphere connection. *Journal of Climate*, 15(14), 1969–1978.

Athanasiadis, P.J., Wallace, J.M. and Wettstein, J.J. (2010) Patterns of wintertime jet stream variability and their relation to the storm tracks. *Journal of the Atmospheric Sciences*, 67(5), 1361–1381.

Baldwin, M.P. and Dunkerton, T.J. (1999) Propagation of the Arctic Oscillation from the stratosphere to the troposphere. *Journal of Geophysical Research: Atmospheres*, 104(D24), 30937–30946.

Barnes, E.A. and Hartmann, D.L. (2010) Influence of eddy-driven jet latitude on North Atlantic jet persistence and blocking frequency in CMIP3 integrations. *Geophysical Research Letters*, 37(23).

Bony, S., Stevens, B., Frierson, D.M.W., Jakob, C., Kageyama, M., PinCUS, R., Shepherd, T.G., Sherwood, S.C., Siebesma, A.P., Sobel, A.H., Watanabe, M. and Webb, M.J. (2015) Clouds, circulation and climate sensitivity. *Nature Geoscience*, 8(4), 261–268.

Ceppi, P. and Hartmann, D.L. (2016) Clouds and the atmospheric circulation response to warming. *Journal of Climate*, 29(2), 783–799.

CIRA (2007). CloudSat ECMWF-AUX auxiliary data process description and interface control document. CIRA, Colorado State University, Fort Collins, CO. Available at: http://www.cloudsat.cira.colostate.edu/sites/default/files/products/files/ECMWF-AUX_PDICD.P_R04.20070718.pdf; accessed 24 February 2020.

Dee, D.P., Uppala, S.M., Simmons, A.J., Berrisford, P., Poli, P., Kobayashi, S., Andrae, U., Balmaseda, M.A., Balsamo, G., Bauer, P., Bechtold, P., Beljaars, A.C.M., van de Berg, L., Bidlot, J., Bormann, N., Delsol, C., Dragani, R., Fuentes, M., Geer, A.J., Haimberger, L., Healy, S.B., Hersbach, H., Hólm, E.V., Isaksen, I., Kållberg, P., Köhler, M., Matricardi, M., McNally, A.P., Monge-Sanz, B.M., Morcrette, J.-J., Park, B.-K., Peubey, C., de Rosnay, P., Tavolato, C., Thépaut, J.-N. and Vitart, F. (2011) The ERA-Interim reanalysis: configuration and performance of the data assimilation system. *Quarterly Journal of the Royal Meteorological Society*, 137, 553–597.

ECMWF (2010). IFS documentation CY36R1, Part IV: physical processes. ECMWF, Reading, UK. Available at: <https://www.ecmwf.int/node/9233>; accessed 24 February 2020.

Fink, A.H., Pohle, S., Pinto, J.G. and Knippertz, P. (2012) Diagnosing the influence of diabatic processes on the explosive deepening of extratropical cyclones. *Geophysical Research Letters*, 39(7). <https://doi.org/10.1029/2012GL051025>.

Greatbatch, R.J. and Jung, T. (2007) Local versus tropical diabatic heating and the winter North Atlantic Oscillation. *Journal of Climate*, 20(10), 2058–2075.

Grise, K.M. and Medeiros, B. (2016) Understanding the varied influence of midlatitude jet position on clouds and cloud radiative effects in observations and global climate models. *Journal of Climate*, 29(24), 9005–9025.

Grise, K.M., Medeiros, B., Benedict, J.J. and Olson, J.G. (2019) Investigating the influence of cloud radiative effects on the extratropical storm tracks. *Geophysical Research Letters*, 46(13), 7700–7707.

Grise, K.M. and Polvani, L.M. (2014) Southern Hemisphere cloud-dynamics biases in CMIP5 models and their implications for climate projections. *Journal of Climate*, 27(15), 6074–6092.

Grise, K.M., Polvani, L.M., Tselioudis, G., Wu, Y. and Zelinka, M.D. (2013) The ozone hole indirect effect: cloud-radiative anomalies accompanying the poleward shift of the eddy-driven jet in

- the Southern Hemisphere. *Geophysical Research Letters*, 40(14), 3688–3692.
- Harries, J.E., Russell, J.E., Hanafin, J.A., Brindley, H., Futyan, J., Rufus, J., Kellock, S., Matthews, G., Wrigley, R., Last, A., Mueller, J., Mossavati, R., Ashmall, J., Sawyer, E., Parker, D., Caldwell, M., Allan, P.M., Smith, A., Bates, M.J., Coan, B., Stewart, B.C., Lepine, D.R., Cornwall, L.A., Corney, D.R., Ricketts, M.J., Drummond, D., Smart, D., Cutler, R., Dewitte, S., Clerbaux, N., Gonzalez, L., Ipe, A., Bertrand, C., Joukoff, A., Crommelinck, D., Nelms, N., Llewellyn-Jones, D.T., Butcher, G., Smith, G.L., Szewczyk, Z.P., Mlynczak, P.E., Slingo, A., Allan, R.P. and Ringer, M.A. (2005) The geostationary earth radiation budget project. *Bulletin of the American Meteorological Society*, 86(7), 945–960.
- Haynes, J.M., Vonder Haar, T.H., L'Ecuyer, T. and Henderson, D. (2013) Radiative heating characteristics of Earth's cloudy atmosphere from vertically resolved active sensors. *Geophysical Research Letters*, 40(3), 624–630.
- Henderson, D.S., L'Ecuyer, T., Stephens, G., Partain, P. and Sekiguchi, M. (2013) A multisensor perspective on the radiative impacts of clouds and aerosols. *Journal of Applied Meteorology and Climatology*, 52(4), 853–871.
- Hurrell, J.W. (1995) Decadal trends in the North Atlantic Oscillation: regional temperatures and precipitation. *Science*, 269(5224), 676–679.
- Hurrell, J.W. and Deser, C. (2010) North Atlantic climate variability: the role of the North Atlantic Oscillation. *Journal of Marine Systems*, 79(3), 231–244.
- Hurrell, J.W., Kushnir, Y., Ottersen, G. and Visbeck, M. (2003). An overview of the North Atlantic Oscillation, Pp. 1–35 in *The North Atlantic Oscillation: Climatic Significance and Environmental Impact*. American Geophysical Union, Washington DC.
- Kidston, J., Scaife, A.A., Hardiman, S.C., Mitchell, D.M., Butchart, N., Baldwin, M.P. and Gray, L.J. (2015) Stratospheric influence on tropospheric jet streams, storm tracks and surface weather. *Nature Geoscience*, 8(6), 433–440.
- Knippertz, P. and Fink, A.H. (2008) Dry-season precipitation in tropical West Africa and its relation to forcing from the extratropics. *Monthly Weather Review*, 136(9), 3579–3596.
- Knippertz, P., Fink, A.H. and Pohle, S. (2009) Reply to comments on 'Dry-season precipitation in tropical West Africa and its relation to forcing from the extratropics'. *Monthly Weather Review*, 137(9), 3151–3157.
- Krahmann, G. and Visbeck, M. (2003) Variability of the Northern Annular Mode's signature in winter sea ice concentration. *Polar Research*, 22(1), 51–57.
- L'Ecuyer, T.S., Wood, N.B., Haladay, T., Stephens, G.L. and Stackhouse Jr., P.W. (2008) Impact of clouds on atmospheric heating based on the R04 CloudSat fluxes and heating rates data set. *Journal of Geophysical Research: Atmospheres*, 113(D8). <https://doi.org/10.1029/2008JD009951>.
- Li, Y. and Thompson, D.W.J. (2016) Observed signatures of the barotropic and baroclinic annular modes in cloud vertical structure and cloud radiative effects. *Journal of Climate*, 29(13), 4723–4740.
- Li, Y., Thompson, D.W.J. and Bony, S. (2015) The influence of atmospheric cloud radiative effects on the large-scale atmospheric circulation. *Journal of Climate*, 28(18), 7263–7278.
- Li, Y., Thompson, D.W.J., Bony, S. and Merlis, T.M. (2019) Thermodynamic control on the poleward shift of the extratropical jet in climate change simulations: the role of rising high clouds and their radiative effects. *Journal of Climate*, 32(3), 917–934.
- Li, Y., Thompson, D.W.J., Huang, Y. and Zhang, M. (2014a) Observed linkages between the Northern Annular Mode/North Atlantic Oscillation, cloud incidence, and cloud radiative forcing. *Geophysical Research Letters*, 41(5), 1681–1688.
- Li, Y., Thompson, D.W.J., Stephens, G.L. and Bony, S. (2014b) A global survey of the instantaneous linkages between cloud vertical structure and large-scale climate. *Journal of Geophysical Research: Atmospheres*, 119(7), 3770–3792.
- Ling, J. and Zhang, C. (2013) Diabatic heating profiles in recent global reanalyses. *Journal of Climate*, 26(10), 3307–3325.
- Loeb, N.G., Doelling, D.R., Wang, H., Su, W., Nguyen, C., Corbett, J.G., Liang, L., Mitrescu, C., Rose, F.G. and Kato, S. (2018) Clouds and the Earth's Radiant Energy System (CERES) energy balanced and filled (EBAF) top-of-atmosphere (TOA) edition-4.0 data product. *Journal of Climate*, 31(2), 895–918.
- Lorenz, D.J. and Hartmann, D.L. (2001) Eddy-zonal flow feedback in the Southern Hemisphere. *Journal of the Atmospheric Sciences*, 58(21), 3312–3327.
- Lorenz, D.J. and Hartmann, D.L. (2003) Eddy-zonal flow feedback in the Northern Hemisphere winter. *Journal of Climate*, 16(8), 1212–1227.
- Mace, G.G., Zhang, Q., Vaughan, M., Marchand, R., Stephens, G., Trepte, C. and Winker, D. (2009) A description of hydrometeor layer occurrence statistics derived from the first year of merged CloudSat and CALIPSO data. *Journal of Geophysical Research: Atmospheres*, 114(D8). <https://doi.org/10.1029/2007JD009755>.
- Maranan, M., Fink, A.H., Knippertz, P., Francis, S.D., Akpo, A.B., Jegede, G. and Yorke, C. (2019) Interactions between convection and a moist vortex associated with an extreme rainfall event over southern West Africa. *Monthly Weather Review*, 147(7), 2309–2328.
- Oreopoulos, L., Cho, N. and Lee, D. (2017) New insights about cloud vertical structure from CloudSat and CALIPSO observations. *Journal of Geophysical Research: Atmospheres*, 122(17), 9280–9300.
- Rutan, D.A., Kato, S., Doelling, D.R., Rose, F.G., Nguyen, L.T., Caldwell, T.E. and Loeb, N.G. (2015) CERES synoptic product: methodology and validation of surface radiant flux. *Journal of Atmospheric and Oceanic Technology*, 32(6), 1121–1143.
- Scaife, A.A., Folland, C.K., Alexander, L.V., Moberg, A. and Knight, J.R. (2008) European climate extremes and the North Atlantic Oscillation. *Journal of Climate*, 21(1), 72–83.
- Schäfer, S.A.K. and Voigt, A. (2018) Radiation weakens idealized midlatitude cyclones. *Geophysical Research Letters*, 45(6), 2833–2841.
- Semenov, V.A. and Latif, M. (2015) Nonlinear winter atmospheric circulation response to Arctic sea ice concentration anomalies for different periods during 1966–2012. *Environmental Research Letters*, 10(5). <https://doi.org/10.1088/1748-9326/10/5/054020>.
- Tanelli, S., Durden, S.L., Im, E., Pak, K.S., Reinke, D.G., Partain, P., Haynes, J.M. and Marchand, R.T. (2008) CloudSat's cloud profiling radar after two years in orbit: performance, calibration, and processing. *IEEE Transactions on Geoscience and Remote Sensing*, 46(11), 3560–3573.

- Thompson, D.W.J., Lee, S. and Baldwin, M.P. (2003). Atmospheric processes governing the Northern Hemisphere Annular Mode/North Atlantic Oscillation, Pp. 81–112 in *The North Atlantic Oscillation: Climatic Significance and Environmental Impact*. American Geophysical Union, Washington DC.
- Tselioudis, G., Lipat, B.R., Konsta, D., Grise, K.M. and Polvani, L.M. (2016) Midlatitude cloud shifts, their primary link to the hadley cell, and their diverse radiative effects. *Geophysical Research Letters*, 43(9), 4594–4601.
- Verlinden, K.L., Thompson, D.W.J. and Stephens, G.L. (2011) The three-dimensional distribution of clouds over the Southern Hemisphere high latitudes. *Journal of Climate*, 24(22), 5799–5811.
- Visbeck, M. (2002) The ocean's role in atlantic climate variability. *Science*, 297(5590), 2223–2224.
- Visbeck, M.H., Hurrell, J.W., Polvani, L. and Cullen, H.M. (2001) The North Atlantic Oscillation: past, present, and future. *Proceedings of the National Academy of Sciences*, 98(23), 12876–12877.
- Voigt, A., Albern, N. and Papavasileiou, G. (2019) The atmospheric pathway of the cloud-radiative impact on the circulation response to global warming: important and uncertain. *Journal of Climate*, 32(10), 3051–3067.
- Voigt, A. and Shaw, T.A. (2015) Circulation response to warming shaped by radiative changes of clouds and water vapour. *Nature Geoscience*, 8(2), 102–106.
- Voigt, A. and Shaw, T.A. (2016) Impact of regional atmospheric cloud radiative changes on shifts of the extratropical jet stream in response to global warming. *Journal of Climate*, 29(23), 8399–8421.
- Wanner, H., Brönnimann, S., Casty, C., Gyalistras, D., Luterbacher, J., Schmutz, C., Stephenson, D.B. and Xoplaki, E. (2001) North Atlantic Oscillation – concepts and studies. *Surveys in Geophysics*, 22(4), 321–381.
- Watt-Meyer, O. and Frierson, D.M.W. (2017) Local and remote impacts of atmospheric cloud radiative effects onto the eddy-driven jet. *Geophysical Research Letters*, 44(19), 10036–10044.
- Woollings, T., Hannachi, A. and Hoskins, B.J. (2010) Variability of the North Atlantic eddy-driven jet stream. *Quarterly Journal of the Royal Meteorological Society*, 136, 856–868.
- Woollings, T., Papritz, L., Mbengue, C. and Spengler, T. (2016) Diabatic heating and jet stream shifts: a case study of the 2010 negative North Atlantic Oscillation winter. *Geophysical Research Letters*, 43(18), 9994–10002.
- Xia, X. and Chang, E.K.M. (2014) Diabatic damping of zonal index variations. *Journal of the Atmospheric Sciences*, 71(8), 3090–3105.
- Zelinka, M.D., Grise, K.M., Klein, S.A., Zhou, C., DeAngelis, A.M. and Christensen, M.W. (2018) Drivers of the low-cloud response to poleward jet shifts in the North Pacific in observations and models. *Journal of Climate*, 31(19), 7925–7947.

SUPPORTING INFORMATION

Additional supporting information may be found online in the Supporting Information section at the end of this article.

How to cite this article: Papavasileiou G, Voigt A, Knippertz P. The role of observed cloud-radiative anomalies for the dynamics of the North Atlantic Oscillation on synoptic time-scales. *Q.J.R. Meteorol. Soc.* 2020;146:1822–1841. <https://doi.org/10.1002/qj.3768>